

PETROLOGY, GEOCHEMISTRY AND GEOCHRONOLOGY OF THE ARQUÍA COMPLEX'S METABASITES AT THE PIJAO-GÉNOVA SECTOR, CENTRAL CORDILLERA, COLOMBIAN ANDES

Carlos Alberto García-Ramírez^{1*}, Carlos Alberto Ríos-Reyes¹, Oscar Mauricio Castellanos-Alarcón²; Luis Carlos Mantilla-Figueroa¹

DOI: <http://dx.doi.org/10.18273/revbol.v39n1-2017005> 

Forma de citar: García-Ramírez, C.A., Ríos-Reyes, C.A., Castellanos-Alarcón, O.M., y Mantilla-Figueroa, L.C. 2017. Petrology, geochemistry and geochronology of the Arquía Complex's metabasites at the Pijao-Génova sector, Central Cordillera, Colombian Andes. *Boletín de Geología*, 39(1): 105-126.

ABSTRACT

Metabasites belonging to the Arquía Complex and outcropping along the Pijao-Génova strip (western edge of the Central Cordillera of the Colombian Andes) consist of chlorite schists, actinolite schists with and without garnet, amphibolites, garnet-amphibolites, eclogites and metabasalts. Some bodies of serpentinized peridotites are observed along with metabasites. Both rock types are confined to the tectonic block bordered by the Cauca-Almaguer and Silvia-Pijao fault systems and their satellite faults. Metabasites were affected by a regional metamorphism, reaching their peak of metamorphism at the amphibolite facies. The Rare Earth Elements (REEs) (normalized to the C1 chondrite) from the studied rocks show a Light REEs depletion and a flat or no-fractionated Heavy REEs patterns. The metabasites' REEs patterns, along with their La/Sm ratio < 0.6 and positive Nb, Ta and Ti anomalies, may suggest their protoliths are MORB-type related. The lithologic association between metabasites, few metapelites and deformed ultramafic rocks suggest that the rocks of the Complex Arquía can represent remnants of an ophiolite sequence of N-MORB type series. The whole rock-garnet Lu-Hf geochronology from metabasites yield an age of 128.7±3.5 Ma. This age has been interpreted as the age at which these rocks reached the eclogite facies, which in turn coincides with the roll-back process of the subducted ocean lithosphere and the Quebradagrande magmatic arc formation.

Keywords: Petrology; metabasites; Arquía Complex; Cordillera Central; Colombia.

PETROLOGÍA, GEOQUÍMICA Y GEOCRONOLOGÍA DE LAS METABASITAS DEL COMPLEJO ARQUÍA EN EL SECTOR PIJAO-GÉNOVA, CORDILLERA CENTRAL, ANDES COLOMBIANOS

RESUMEN

Las metabasitas del Complejo Arquía en la franja Pijao-Génova, borde occidental de la Cordillera Central de los Andes Colombianos, consisten en esquistos cloríticos, esquistos actinolíticos con y sin granate, anfíbolitas, anfíbolitas granatíferas, eclogitas y metabasaltos. Algunos cuerpos de peridotitas serpentinizadas afloran a lo largo de fallas del sistema Cauca-Almaguer y Silvia-Pijao, así como sus fallas satélites. Las metabasitas fueron afectadas por un metamorfismo regional, alcanzando su pico metamórfico en facies anfíbolita. Los elementos de tierras raras (ETRs) (normalizados al condrito C1) de las rocas estudiadas muestran un empobrecimiento en ETRs Ligeros y patrones planos a poco fraccionados de ETRs Pesados. Los patrones de ETRs de las metabasitas, junto con su relación La/Sm < 0.6 y anomalías positivas en Nb, Ta y Ti, pueden sugerir que sus protolitos son de tipo MORB. La asociación litológica entre metabasitas, escasas metapelitas y rocas ultramáficas deformadas proponen que las rocas del Complejo Arquía podrían constituir remanentes de una secuencia ofiolítica de series tipo N-MORB. La geocronología Lu-Hf en roca total-granate de las metabasitas produjo una edad de 128.7±3.5 Ma. Esta edad se ha interpretado como la edad en que estas rocas alcanzaron la facies eclogita, que a su vez coincide con el proceso de *roll-back* de la litosfera oceánica subducida y la formación del arco magmático de Quebradagrande.

Palabras clave: Petrología; metabasitas; Complejo Arquía; Cordillera Central; Colombia.

¹ Escuela de Geología, Universidad Industrial de Santander, Bucaramanga, Colombia. (*) cgarciar@uis.edu.co, carios@uis.edu.co, lcmantil@uis.edu.co

² Programa de Geología, Universidad de Pamplona, Pamplona, Colombia. oscarcmca@yahoo.es

INTRODUCTION

Northern Andes have lithogeologic and tectonostratigraphic characteristics that differentiate them from those of Central and Southern Andes. The NW margin of South America in Colombia is represented by the western edge of the Central and Western cordilleras, the Cauca-Patia Valley, and the Choco-Panamá terrain. These regions are the result of processes of accretion and amalgamation to the South American margin of Mesozoic rocks formed in ocean environments, such as island arcs, oceanic plateaus and mid-ocean ridges (Kerr *et al.*, 1997; Moreno-Sánchez and Pardo-Trujillo, 2003; Pindell and Kennan, 2009; Cediel *et al.*, 2003; Villagómez *et al.*, 2011; Ruiz *et al.*, 2012; Bustamante *et al.*, 2011). The limit of the continental and oceanic crust in Colombia has been previously discussed as the Cretaceous boundary in the western Colombia, which has been defined by the Cauca-Almaguer fault system. However, further east protoliths of oceanic affinity for metabasites of the Arquía Complex and volcanic rocks of the Quebradagrande Complex (Ruiz *et al.*, 2012; Villagómez *et al.*, 2011; Rodríguez and Arango, 2013). Currently, the terrains located between the Cauca-Almaguer San Jerónimo faults are considered as the Romeral Melange (Cediel *et al.*, 2003), where thin and discontinuous tectonic blocks of oceanic and continental origin are located (Rodríguez and Arango, 2013). Therefore, the current geological setting involving autochthonous, paraautochthonous and allochthonous terrains, which has hindered their understanding and definition as lithostratigraphic or lithotectonic units Villagómez *et al.* (2011). This study provides new petrology, geochemistry and geochronology data of the metabasites from the Arquía Complex in the sector Pijao-Génova, Central Cordillera, Colombia, which can provide useful information about the magmatic precursors and their geotectonic setting of formation.

GEOLOGICAL SETTING

The Arquía Complex is a strip of metamorphic rocks that are located on the west side of the Central Cordillera and is limited by the Cauca-Almaguer Fault on the west and Silvia-Pijao Fault on the east. It consists of metagabroic rocks, garnet amphibolites, amphibole schists, quartz-sericite schists and quartzites of medium- to low-pressure, as well as lawsonite and glaucophane schists and eclogites of high pressure and serpentinized ultramafic rocks (Maya and González,

1995). The geological units constituting the Arquía Complex comprise from north to south: Sabaletas Schists, Arquía Group, Lisboa-Palestine Schists, Bolo Azul complex, Río Rosario Complex, Bugalagrande Group, Barragan Schists, Jambaló Schists and Buesaco Metamorphites. Moreno-Sánchez and Pardo-Trujillo (2003) propose naming it as Arquía-Guamote Complex by its similarity with medium- to high-pressure rocks outcropping in Ecuador as in a thin strip of blueschists and eclogites of the Raspas Complex and quartzites and phyllites of the Guamote Division bounded on the east by the Peltec Fault. Villagómez *et al.* (2011) states that the Arquía and Raspas complexes are similar because both sequences have been tectonically juxtaposed against an arch, are strongly foliated and are located in an area of suture formed by the accretion of the Caribbean Large Igneous Province (LIP). Different geochemical studies on the rocks of the Arquía Complex reveal an oceanic origin from tholeiitic basalts in MORB or N-MORB environments types (Villagómez *et al.*, 2011; Rodríguez and Arango, 2013; Ruiz *et al.*, 2012). The behavior of Rare Earth Element (REEs) show a depletion in light REEs (LREEs) and a nearly flat bit fractional behavior of the heavy REE (HREE) with similar relations for the $(La/Sm)_N < 0.6$ with absence of negative anomalies in Nb, Ta and Ti. Villagómez *et al.* (2011) attribute this behavior to subduction-related processes. Rodríguez and Arango (2013), considering the lithological association between deformed metabasites, scarce metapelites and ultramafic rocks, suggest that the Arquía Complex's rocks can represent remnants of an ophiolite sequence of the N-MORB type series. The conditions of metamorphism of the metabasites of the Arquía Complex in all lithotypes studied along the Central Cordillera reached the amphibolite facies for the garnet-amphibolite without garnet and greenschist facies for the epidote actinolite schists. Ruiz (2013), in the Arquía Complex's rocks located between Santa Fe de Antioquia on the north and the Arquía river on the south, determined to pressure and temperature conditions of 10.2 kb at 640°C for amphibolites and 7.2 kb at 430°C for schists by geothermobarometric calculations, using the Perplex software.

The PT path of these rocks is clockwise. The age of the Arquía Complex is still uncertain. Rodríguez and Arango (2013) compiled and discussed the meaning of the ages obtained in the Arquía Complex's rocks, highlighting two main age ranges: 203-229 and 100-113 Ma. The first of them can be associated with the age of metamorphism of the Arquía Complex's

rocks, suggesting that some of these rocks form a complex melange in the suture zone between the eastern San Jerónimo and western Cauca-Almaguer faults. The second of them can be associated with the development of the regional Barroso-Sabanalarga volcanic-plutonic arch, which extends from the Lower to the Middle Cretaceous. The age of the metamorphism of the Arquía Complex in recent years has been defined by Villagómez *et al.* (2011) and Ruiz (2013). Ar/Ar ages between 117-107 Ma indicate post-peak metamorphic cooling ages and are compared to the age of 130 Ma defined for the metamorphism of the Raspas Complex in Ecuador (Villagómez *et al.*, 2011). Ruiz (2013) reports an amphibole Ar/Ar plateau age of 106.9 Ma, which attributes as the cooling age after the metamorphic peak. The numerous reported ages for the Arquía Complex's rocks do not allow a unanimous interpretation with respect to their significance in the regional context of the Northern Andes (Rodríguez and Arango, 2013). This is due primarily to the geological-structural position of these rocks as discontinuous tectonic blocks in a suture zone with tectonic boundaries with the adjacent units. On the other hand, the methods and dated materials (whole rock, mineral) are very diverse and, therefore, may reveal different ages the age of the protolith, the age of emplacement, the age of metamorphism, the age of metamorphic post-peak or the age of collision/accretion. The Arquía Complex's rocks in the study area are located between Pijao and Génova municipalities (FIGURE 1) and comprise the geological units denominated by McCourt *et al.* (1985) as Bugalagrande Group and El Rosario Complex. The Bugalagrande Group is composed of chlorite and actinolite schists interlayered with pelitic schists and quartzites, while El Rosario Complex consists of amphibolites and garnet amphibolites with weak- to well-developed foliation. Associated to these rocks are lenticular bodies of serpentinized and mylonitized ultramafic rocks along the Silvia-Pijao Fault.

Here, different ages are reported for the Arquía Complex's rocks. Toussaint and Restrepo (1978) dated a garnet amphibolite by whole rock K/Ar, obtaining an age of 110 Ma. Ages hornblende K/Ar in amphibolites of El Rosario Complex are in the range 94-115 Ma McCourt *et al.* (1984). Villagómez (2010) reports Ar/Ar ages ranging between 117 and 107 Ma. In contrast to other sectors, where the Arquía Complex's rocks have been dated, less variation in ages for the sector Pijao-Génova can be observed.

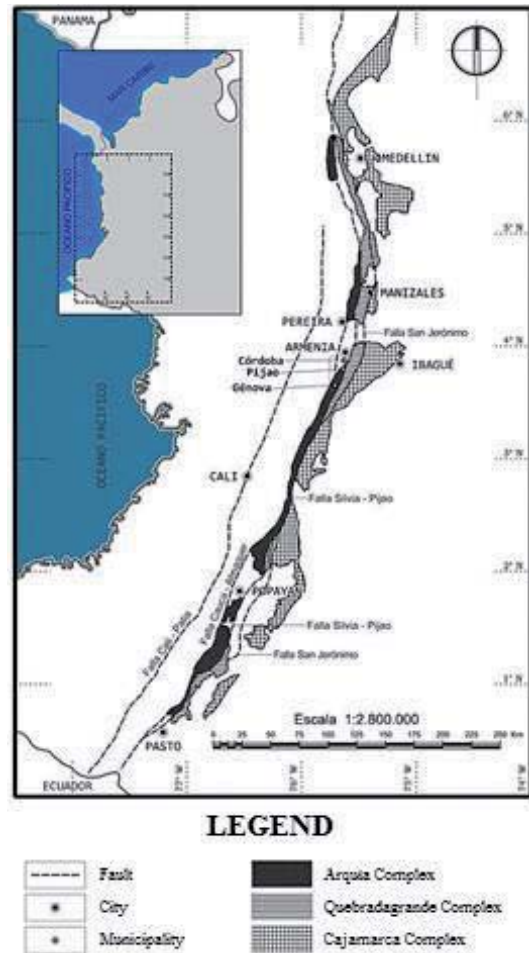


FIGURE 1. Geographical distribution of the geological units of the Arquía Complex and its adjacent complexes: (1) Sabaleta Schists; (2) Arquía Group; (3) Lisboa-Palestina Schists; (4) Rosario Group; (5) Bugalagrande Group; (6) Boloazul Complex; (7) Blueschists Belt; (8) Buesaco metamorphic sequence. Source: Adapted and modified from Moreno-Sanchez and Pardo-Trujillo, (2003).

ANALYTICAL TECHNIQUES

A research team of the School of Geology (Universidad Industrial de Santander) performed several fieldworks on the Arquía Complex cropping out between Pijao and Génova at the Central Cordillera (Colombia) to collect metabasites and associated rocks from several outcrops in fresh roadcuts and new quarries along the roads. The petrographic analysis was performed on polished thin sections, using a Leica DM750P microscope of the Universidad Industrial de Santander and an Olympus BX-51 microscope of the Universidad de Pamplona. Mineral abbreviations are after Whitney and Evans (2010). Whole-rock major and trace elements were analyzed at Acme Analytical Laboratories Ltd., Vancouver, Canada. The detailed

analytical conditions and procedure are as follows: 250 g of rock were crushed, split and pulverized to 200 mesh; FeO was obtained by titration 0.5 (AcmeLabs, 2015). Rock samples were crushed in steel crushers and grinded in an agate mill to a grain size of < 200 mesh. Major elements were determined by wavelength dispersive sequential X-ray fluorescence (WDSXRF) spectrometry, whereas trace elements were determined by ICP mass spectrometry (ICP-MS). The geochemical data processing was performed using the computer program Geochemical Data Toolkit (GCDKit) version 3.00 by Janoušek *et al.* (2006). A sample of eclogite (ARQ-359) from the Arquía Complex in the area of interest was selected for Lu–Hf garnet geochronology, with multiple garnet and whole-rock fractions, each consisting of 200–250 mg of material, which were dissolved in the radiogenic isotope clean laboratory at Washington State University according to the standard protocol described by Nesheim *et al.* (2012). The protocols for dissolution, spiking, chemical separations, and analyses used in garnet Lu–Hf geochronology are fully discussed in Cheng *et al.* (2008). The protocol used for separation of Lu and Hf is based on procedures described by several authors (Cheng *et al.*, 2008; Patchett and Tatsumoto, 1981; Vervoort and Patchett, 1996; Münker *et al.*, 2001). Lu–Hf isotopic analyses were conducted on a ThermoFinnigan™ Neptune MC-ICP-MS at Washington State University. The description of chemical sample treatment is presented in Vervoort *et al.* (2004) and Bouvier *et al.* (2008). The linear regression for the Lu–Hf errorchron was calculated using Isoplot/Ex Ludwig (2003) and a ^{176}Lu decay constant of 1.867×10^{-11} (Scherer *et al.*, 2001; Söderlund *et al.*, 2004).

FIELD OCCURRENCE

Metabasites and associated rocks in the study area occur as scarce intercalations of variable morphology and thickness, developing discontinuous bands and lenticular bodies, most of them affected by tectonism, within the metamorphic sequence of the Arquía Complex at the Central Cordillera. These rocks are composed mainly of chlorite and actinolite to amphibole schists, the last of them with or without garnet, with minor amphibolites and garnet-bearing amphibolites and subordinate amounts of eclogites, serpentized peridotites and metabasalts.

Olive green chlorite schists (FIGURE 2a) crop out to the northwest of Génova, displaying a plane parallel

schistosity defined primarily by chlorite. Locally, they show a crenulated structure. Green to gray-green actinolite schists (FIGURE 2b) crop out to the south of Génova and on the road from this municipality to Barragan. These rocks show a very well-developed foliation with a plane parallel geometry, which is defined by the preferred orientation of chlorite and actinolite. In some cases, they show a crenulated structure or weak to intense deformation superimposed to the main foliation of the rock, developing a mylonitic structure characterized by the presence of thin strips of elongated quartz and actinolite, intercalated with thick bands of quartz and plagioclase. Green to brownish green garnet-bearing amphibole schists (FIGURE 2c) are exposed on the road from Génova to Barragan and near Córdoba. These rocks exhibit a schistose structure defined by the alignment of amphibole. They show jointing and intense fracturing, deformation and deflection of the main foliation of the rock around most garnet porphyroblasts. In some cases, a strong mylonitic deformation evidenced by lengthening and stretching of quartz, among others, is observed. Green amphibolites are exposed on the roads from Pijao to Cordoba and Buenavista. These rocks exhibit a plane parallel to lightly wavy structure and intense jointing and fracturing. In general, they show a weak foliation. In some cases, abundant quartz veins up to 1 cm of thickness and tabular geometry occur parallel to the main foliation of the rock. However, quartz veins also occur cutting obliquely or perpendicularly this foliation. Dark green to light green garnet amphibolites (FIGURE 2e) crop out on the roads from Pijao to Buenavista and Puente Tabla. These rocks have a banded to massive structure. The compositional banding is reflected by alternating nematoblastic (hornblende) and granoblastic (plagioclase) bands, within which epidote-group minerals and garnet porphyroblasts occurs. Locally, a mylonitic deformation is observed, with brittle deformation superimposed. A well-exposed outcrop of eclogites occurs on southwestern of Pijao.

These eclogitic rocks have experienced extensive retrogression after high-P metamorphism. They form meter scale bodies of lenticular geometry enveloped by garnet-bearing amphibolites and locally actinolite schists. Mineral lineations are mainly defined by hornblende and stretching lineations defined by aggregates of quartz and feldspar. The serpentized peridotites (FIGURE 2d) are part of tectonic slices of oceanic crust that occur as lenticular bodies striking NNE-SSW associated to the Silvia-Pijao fault system on the roads from Río Verde to Cordoba and from Pijao

to Río Azul as well as on the margin of the Arenales stream. However, their occurrence is not homogeneous and its spatial distribution is controlled by the complex tectonic environment of the study area. Grayish green

metabasalts crop out to the SE of Génova, particularly in the Río Gris stream, displaying a weak foliation, which is defined by the orientation of the chlorite.

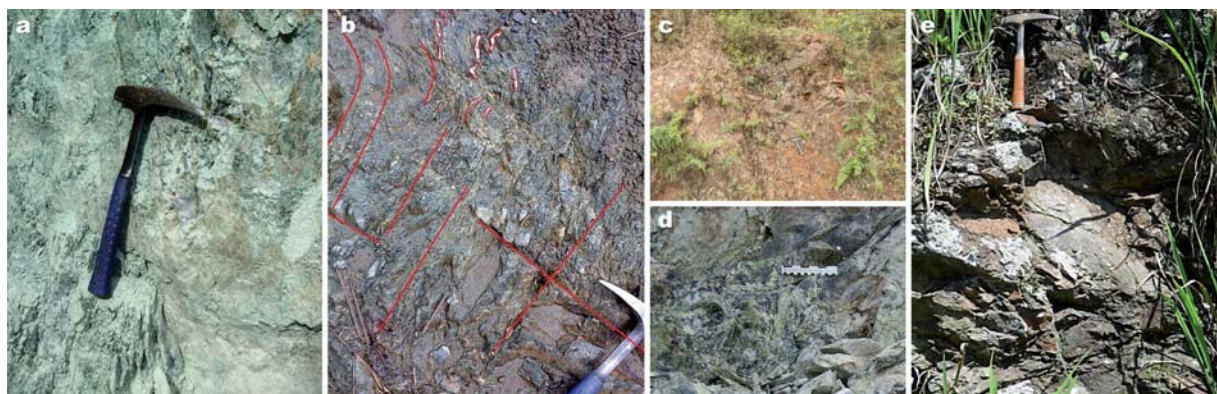


FIGURE 2. Outcrop features of metabasites and associated rocks of the Arquía Complex.

PETROGRAPHY

Metabasites and associated rocks of the Arquía Complex in the study area are mainly represented by chlorite and actinolite to amphibole schists, the last of them with or without garnet porphyroblasts, with minor garnet-bearing or -absent amphibolites and subordinate amounts of serpentinized peridotites and metabasalts. They usually reveal deformations associated to regional major structures, such as the Romeral and Silvia-Pijao fault systems and satellite faults associated to them. The mineralogical varieties of each of these lithotypes are described as follows.

Chlorite schists

The chlorite schists have a schistose structure defined primarily by chlorite and a granolepidoblastic and locally poikiloblastic texture. In some cases, crenulations and “kink” bands in chlorite are recognized. These rocks are mainly composed of chlorite, plagioclase, clinozoisite and quartz. Chlorite (48%) occurs in leafy aggregates evenly distributed, defining the foliation of the rock and presents inclusions of titanite, clinozoisite and quartz. Plagioclase (23%) occurs as heteroblastic and xenoblastic individuals, some of them displaying simple twinning and skeletal forms. It contains numerous inclusions of clinozoisite, titanite and quartz, which follow the direction of the main foliation of the rock. Clinozoisite (13%) develops heteroblastic and xenoblastic individuals arranged in the same direction of the main foliation; it usually presents fractures. Quartz (10%) forms heteroblastic and xenoblastic individuals; it presents inclusions of

titanite, clinozoisite and epidote. A second generation of quartz develops mineral veins. Titanite (3%) occurs as reddish brown and very high relief fine-grained granular aggregates or inclusions. Graphite (2%) occurs as black xenoblasts, developing fine scales in the direction of the main foliation or sometimes microfolds. Opaque (2%) minerals form elongated individuals (FIGURE 3).

Actinolite schists

Actinolitic schists exhibit a marked foliation, which is defined by the preferred orientation of chlorite and actinolite. They show granoblastic and locally porphyroblastic and poikiloblastic textures. In some cases, crenulations, kink bands in chlorite, and weak to intense deformation superimposed to the main foliation of the rock, developing a mylonitic texture characterized by the presence of thin strips of actinolite and elongated quartz, intercalated with thicker bands quartz and plagioclase. Oxidation is observed in fractures in some mineral phases. Petrographically, these rocks vary from actinolite schists to epidote-bearing actinolite schists, quartz-actinolite schists, epidote-bearing quartz-actinolite schists and epidote-bearing tremolite-actinolite schists. They mainly consist of actinolite, chlorite, clinozoisite and quartz, plagioclase and muscovite as minor phases, and epidote and sphene as accessory minerals. Actinolite (35%) occurs defining the S_n and S_{n+1} foliations as elongated prismatic to tabular individuals of subidioblastic and heteroblastic character, with pale green color and slight pleochroism from yellowish green to bluish green.

It presents reaction textures with titanite, epidote and clinozoisite, and inclusions of titanite. Locally microfolds and occasionally fractures are observed. Actinolite shows weak to moderate replacement to chlorite. Chlorite (15%) occurs as colorless to pale green and anomalous interference colors individuals of subidioblastic character, which develop leafy aggregates. A second generation of chlorite is observed at the edges of actinolite. It sometimes presents kink bands. Clinozoisite (12%) defines the S_n and S_{n+1} foliations, developing colorless columnar individuals of irregular borders, and xenoblastic and heteroblastic character. It displays anomalous interference colors, defining a concentric zonation. It presents inclusions of titanite and epidote, which are oriented in the same direction of the external foliation. Quartz (8%) forms colorless individuals with irregular edges of heteroblastic and xenoblastic character, defining the S_n and S_{n+1} foliations, and locally revealing recrystallization phenomena. This mineral sometimes displays wavy extinction. It presents inclusions of titanite, epidote and clinozoisite, which are oriented in the same direction of the external foliation. A second generation of quartz corresponds to fine-grained, euhedral, equigranular and very clean individuals of hydrothermal origin, which is developing veins up to 0.2 mm of thickness. Plagioclase (10%) occurs as colorless individuals of xenoblastic and heteroblastic character, exhibiting polysynthetic twinning. It presents inclusions of epidote, titanite and clinozoisite oriented in the same direction of the external foliation.

A moderate replacement to sericite is frequently observed. Tremolite (6%) develops very fine-grained fibrous aggregates, consisting of tiny idioblastic and homeoblastic individuals, defining the S_n and S_{n+1} foliations. It presents inclusions of epidote and shows incipient alteration to chlorite, which is presented as leafy aggregates of pale green color growing from the edges toward the center of tremolite. Epidote (5%) occurs either as inclusions in actinolite or as partial replacement product of clinozoisite and plagioclase. Rutile (1%) occurs as heteroblastic and subidioblastic individuals (included in titanite and actinolite) of coppery red color, but also developing reaction textures with titanite. Titanite (2%) occurs as individuals of arrow-edge shape of idioblastic character in the rock matrix. A second generation corresponds to granular titanite formed from rutile. This mineral exhibits a reddish brown color and extreme interference colors, which are masked by its color. Muscovite (3%)

develops laminar colorless individuals (straight and splintery edges), which show excellent exfoliation in one direction and interference colors of third order. It presents mottled appearance close to the extinction position. Calcite (5%) occurs as isolated heteroblastic and xenoblastic individuals, of variable relief, rhombohedral exfoliation and extreme birefringence. It presents inclusions of quartz, epidote and titanite. It shows a dissolution texture at its edges. Actinolite schists reveals two events of deformation, the first of them developed the oldest foliation (S_n) defined by actinolite, clinozoisite and quartz, and the second of the developed the main foliation (S_{n+1}) defined by actinolite, quartz, clinozoisite and plagioclase (FIGURE 4).

Garnet-bearing amphibole schists

Garnet-bearing amphibole schists exhibit schistose structure defined by the alignment of actinolite, hornblende and chlorite and granoblastic and locally porphyroblastic and poikiloblastic textures. They sometimes exhibit intense fracturing, deformation and deflection of the outer foliation around most garnet porphyroblasts. In some cases, strong mylonitic deformation evidenced among others by lengthening and stretching of quartz is observed. The deformation in chlorite indicates that the deformation event occurred subsequent to step down. These rocks are mineralogically composed of amphibole (actinolite and hornblende), quartz, garnet, clinozoisite, plagioclase, epidote, titanite and rutile. Actinolite (29%) occurs as elongated tabular to prismatic individuals of subidioblastic and homeoblastic character. It shows olive green color and slight pleochroism from pale green to blue-green color. It contains inclusions of epidote, titanite and clinozoisite. This mineral occurs in two generations, defining the S_{n+1} and S_{n+2} foliations. It presents intense alteration to chlorite. Hornblende (10%) of heteroblastic and subidioblastic character occurs in individuals of pale green color and intense pleochroism from yellow-green to blue-green color. Clinozoisite (8%) presents inclusions of rutile arranged in the same direction of the main foliation. Garnet (15%) exhibits a pre-tectonic character and without-tectonic fractures which have been promoting the circulation of fluids and its gradual replacement by chlorite. It occurs as idioblastic and xenoblastic porphyroblasts of pinkish color. It presents inclusions quartz, clinozoisite, epidote and titanite randomly arranged. Deflection is observed in the external foliation around garnet due to its pre-tectonic character. In other cases, garnet exhibits a sigmoidal pattern of inclusions of quartz, clinozoisite, titanite and epidote, which is

continuous with the direction of the external foliation S_{n+2} , showing non-tectonic character, from which the porphyroblasts of garnet grown defining the foliation S_{n+2} . This mineral displays chloritization at its edges or along fractures. Quartz (14%) occurs in two generations as fine- to medium-grained individuals of irregular borders, which are of xenoblastic and heteroblastic character and elongated in the direction of the main foliation, either as inclusions in some pre-tectonic garnet porphyroblasts or developing the foliation S_{n+2} . It presents inclusions of epidote and titanite, which are arranged in the same direction of the external foliation. Plagioclase (12%) occurs as heteroblastic and xenoblastic individuals, sometimes with simple twinning and incipient alteration to epidote or sericite. Clinozoisite (8%) is characterized by concentric zoning of the anomalous interference colors. It occurs in two generations, either as heteroblastic individuals and idioblastic to xenoblastic individuals, which are broken and elongated in the direction of the main foliation of

the rock (S_{n+2}). It contains inclusions of quartz, epidote and rutile, and is included in pre-tectonic garnet. It is sometimes moderately replaced by epidote to its core. Epidote occurs as individuals of heteroblastic to homeoblastic and subidioblastic character, which are fractured. It shows slight pleochroism from yellowish green to colorless, as inclusions in garnet pre-tectonic porphyroblasts developing the oldest foliation (S_n) and defining the foliation S_{n+2} . Titanite (2%) occurs as heteroblastic and subidioblastic with irregular shapes and brown color, defined as pre-tectonic inclusions in garnet or developing the main foliation. Occasionally textures reaction develops around rutile. Rutile occurs as individuals of heteroblastic and subidioblastic character and reddish brown color, which is masked by its birefringence. Usually it occurs in the same direction of the main foliation. Muscovite (2%) occurs as heteroblastic and subidioblastic individuals of tabular form (FIGURE 5).

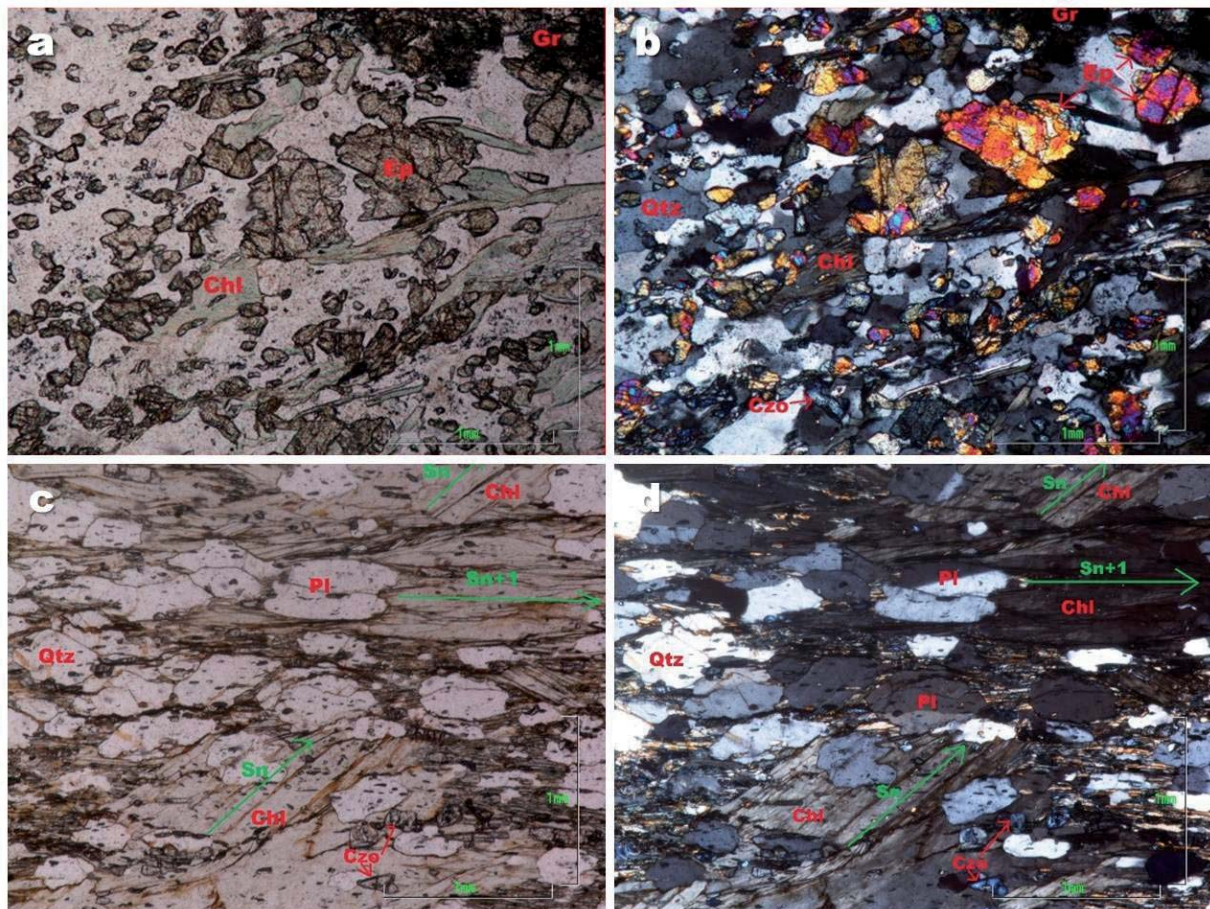


FIGURE 3. Photomicrograph of chlorite schists, displaying their main textural and microstructural features. Chl, chlorite; Pl, plagioclase; Qtz, quartz; Czo, clinozoisite; Ep, epidote; Cal, calcite; Ttn, titanite; Rut, rutile.

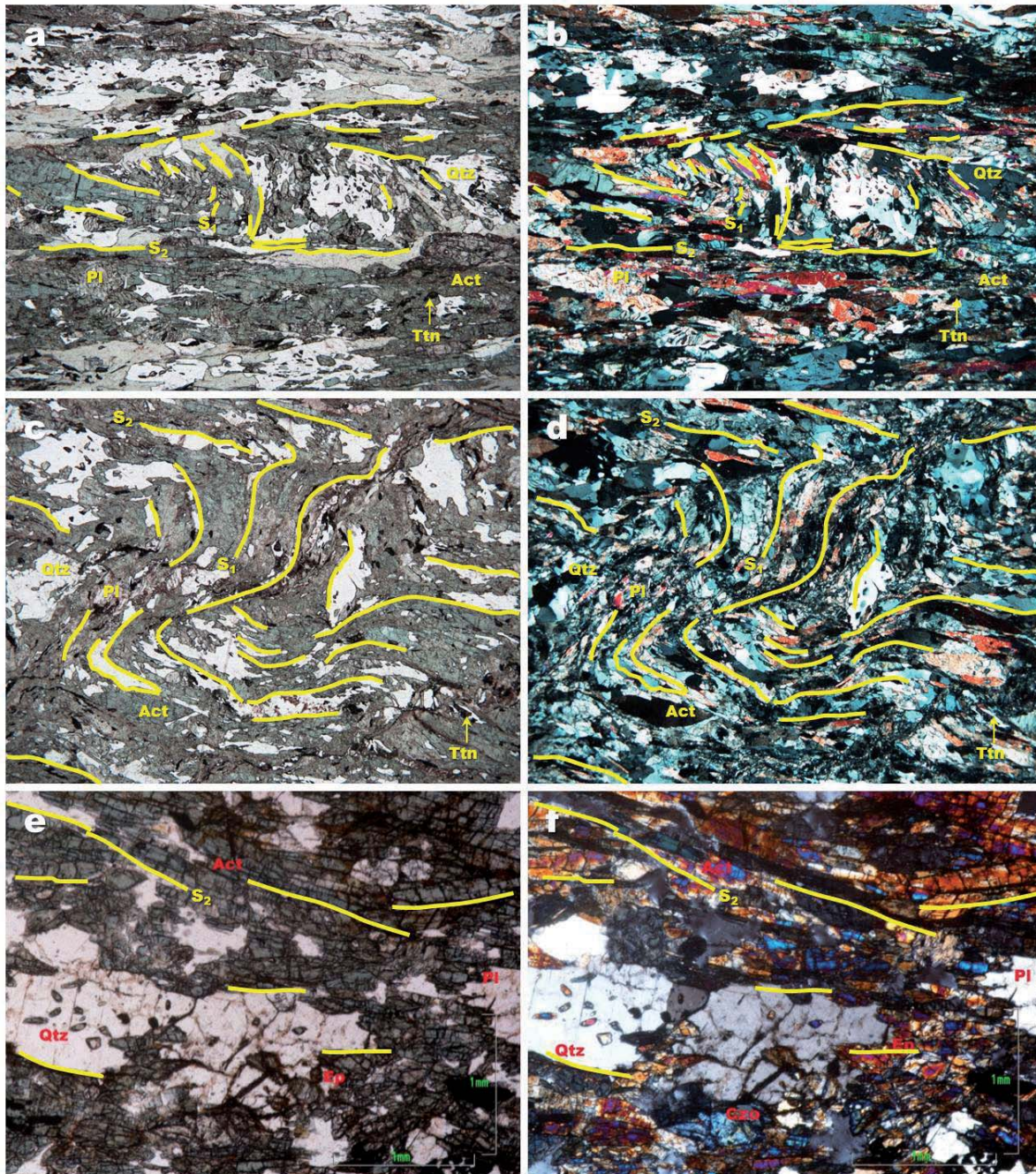


FIGURE 4. Photomicrograph of actinolite schists, displaying their main textural and microstructural features. Act, actinolite; Chl, chlorite; Pl, plagioclase; Qtz, quartz; Czo, clinozoisite; Ep, epidote; Cal, calcite; Ttn, titanite; Rut, rutile.

Amphibolites

Amphibolites exhibit parallel flat to slightly undulating structure and granoblastic texture, as well as intense jointing and fracturing. They show dark green color and are mainly composed of hornblende and plagioclase, with minor amounts of quartz, clinozoisite, titanite and epidote. In general, these rocks exhibit weak foliation, although in some cases hornblende is elongated, defining the foliation

of the rock. In some cases, abundant quartz veins of tabular geometry and up to 1 cm thick are usually arranged parallel to the foliation of these rocks, but also they can occur obliquely crossing and perpendicular this foliation. Hornblende (48%) forms heteroblastic and subidioblastic individuals, strongly fractured, of tabular-prismatic shape with intense pleochroism varying shades of green to brown. It presents inclusions of titanite, clinozoisite

and epidote. Plagioclase (35%) forms heteroblastic and xenoblastic individuals with polysynthetic twinning. It contains inclusions of clinozoisite and titanite, which do not follow a defined pattern. Some plagioclase individuals can be elongated locally defining a preferred direction. It sometimes shows moderate to strong replacement to sericite. Clinozoisite (5%) forms heteroblastic and xenoblastic individuals, usually fractured, with concentric zoning of the anomalous interference colors. Quartz

(6%) occurs in xenoblastic and heteroblastic individuals. It presents inclusions of epidote and titanite. Titanite (4%) form homeoblastic and subidioblastic pale brown individuals, displaying the typical diamond shape and exfoliation in one direction. It presents inclusions of epidote. Epidote (2%) form heteroblastic to homeoblastic and xenoblastic individuals with exfoliation in one direction and birefringence of the third order. This mineral can occur as inclusions in plagioclase and hornblende (FIGURE 6).

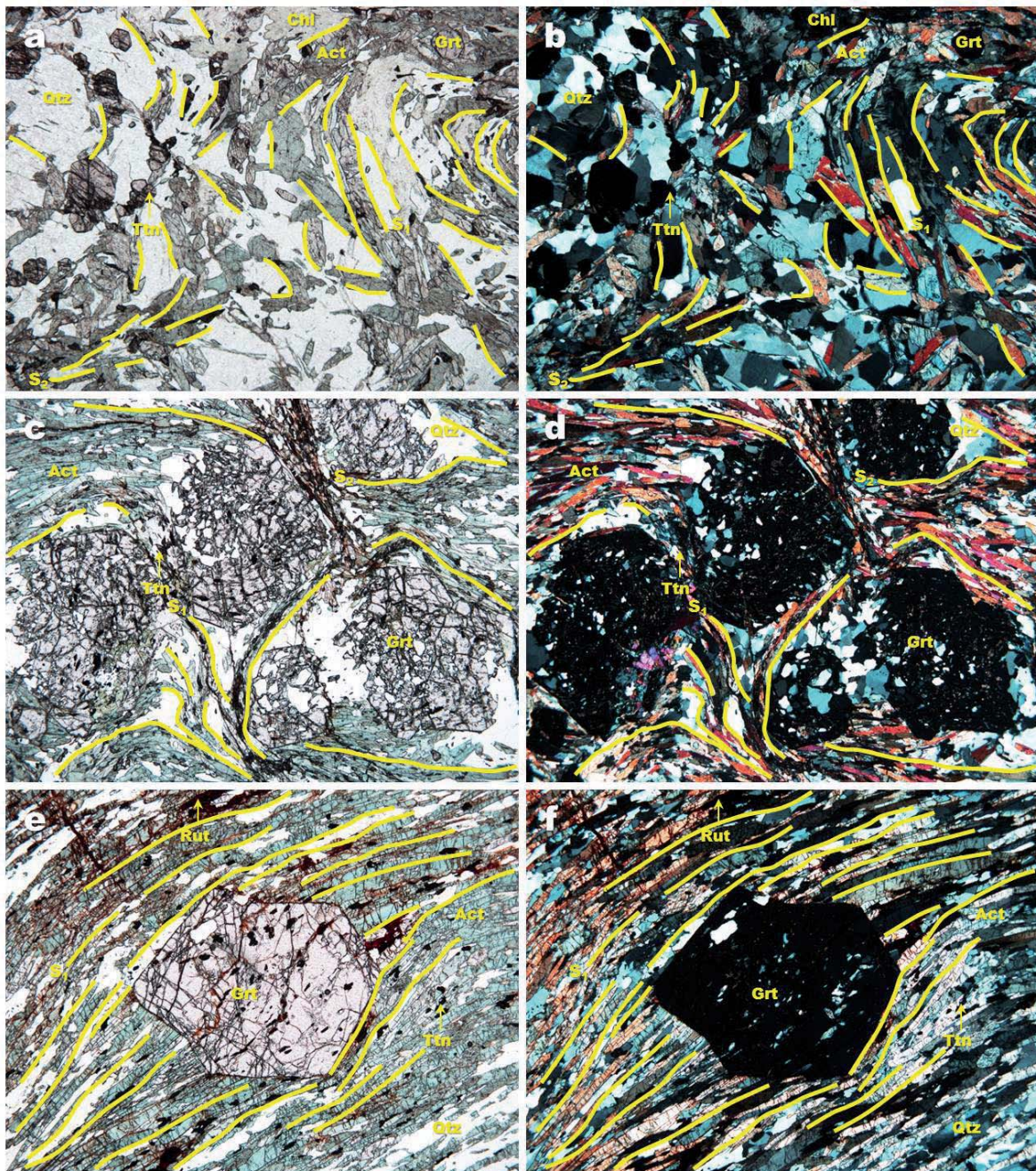


FIGURE 5. Photomicrograph of garnet-bearing actinolite schists, displaying their main textural and microstructural features. Act, actinolite; Chl, chlorite; Pl, plagioclase; Grt, garnet; Qtz, quartz; Czo, clinozoisite; Ep, epidote; Cal, calcite; Ttn, titanite; Rut, rutile.

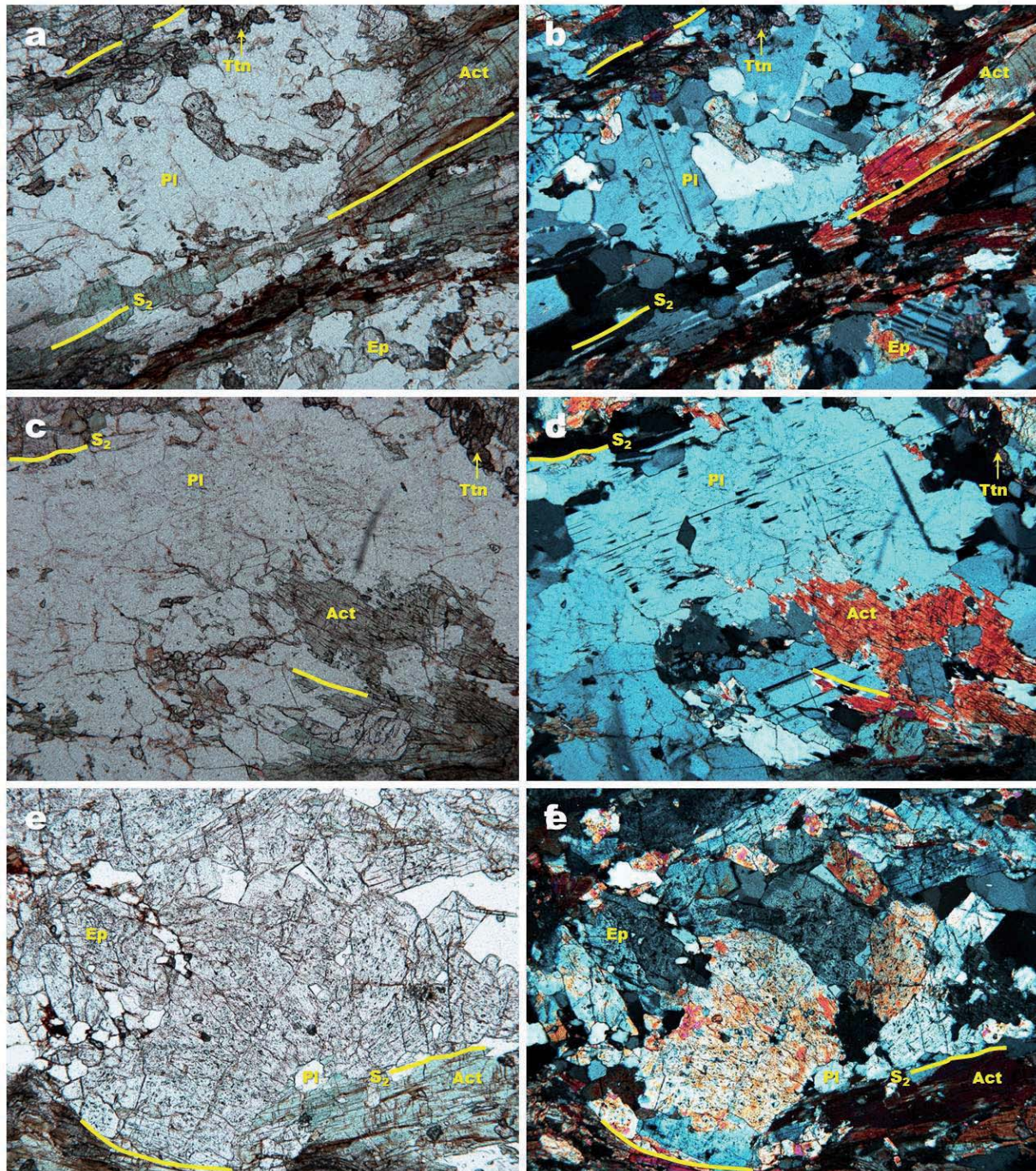


FIGURE 6. Photomicrograph of amphibolites, displaying their main textural and microstructural features. Act, actinolite; Pl, plagioclase; Ep, epidote; Ttn, titanite.

Garnet amphibolites

Garnet amphibolites display banded to massive structure and granoblastic and locally porphyroblastic textures. The compositional banding is reflected in alternating hornblende-bearing nematoblastic and plagioclase-bearing granoblastic bands, within which

epidote-group minerals and garnet porphyroblasts occur. These rocks show dark to light green color and their minerals exhibit evidence of recrystallization and some are fractured. Most of these rocks have fractures perpendicular to the orientation of minerals which are usually filled with calcite.

Locally, mylonitic deformation is observed, with superimposed brittle deformation which mainly affected minerals such as quartz, plagioclase and hornblende, and “kink” bands in plagioclase. Hornblende (35%) occurs as heteroblastic and subidioblastic and strongly fractured individuals of prismatic-tabular shape, pleochroism from brownish green to bluish green. It contains inclusions of clinozoisite, titanite and epidote. Hornblende shows incipient alteration to chlorite. Plagioclase (20%) forms heteroblastic and xenoblastic individuals of skeletal (due to dissolution) and locally poiquiloblastic (due to inclusions of clinozoisite, titanite, hornblende and epidote) character, which are characterized by polysynthetic twinning. It exhibits moderate to strong alteration to sericite and sometimes to epidote or clinozoisite, which develops with a mottled appearance and sometimes from the core of plagioclase. In some cases, this mineral presents “kink” bands as evidence of deformation. Garnet (20%) occurs as fractured pinkish idioblastic to xenoblastic porphyroblasts of average diameter up to 5 mm and skeletal to poiquiloblastic character. It presents a pattern of inclusions of quartz, zoisite, clinozoisite, titanite and rutile, which is concordant with the external foliation, revealing its non- tectonic character. This mineral shows partial and incipient replacement to chlorite and epidote, respectively. Epidote (5%) occurs in two generations, as idioblastic to xenoblastic (with curved edges) and heteroblastic individuals or as a result of partial replacement of plagioclase and garnet. This mineral shows pleochroism and concentric zoning and interference colors. Clinozoisite (8%) forms xenoblastic to subidioblastic and heteroblastic individuals, showing concentric zoning of its anomalous interference colors. Zoisite (4%) occurs in subidioblastic to xenoblastic and heteroblastic individuals of elongated prismatic character and anomalous interference colors. Quartz (5%) occurs as xenoblasts of irregular edges having inclusions of epidote, titanite and clinozoisite. Titanite (2%) occurs as homeoblastic and subidioblastic individuals of arrowhead shape and brown color. A second generation develops granular aggregates of fine-grained reaction rims around rutile. Rutile (1%) forms subidioblastic and heteroblastic individuals of reddish brown color, which is masked by its birefringence. This mineral usually displays reaction textures (titanite after rutile) (FIGURE 7).

Eclogites

Eclogites are fine-grained rocks consisting of garnet porphyroblasts set in a matrix of omphacite (25%), amphibole (hornblende or barroisite) (20%), plagioclase

and zoisite; rutile often rimmed by titanite occurs as the main accessory mineral phase, phengite is quite rare whereas quartz is nearly absent. In general, they show high-P mineralogy with omphacite, garnet, rutile and zoisite. These rocks are characterized by the local occurrence of fine-grained symplectitic textures, which appear as strongly lobate vermicular forms, with each lobe showing an optical continuity with its parent grain. Relicts of the eclogite facies metamorphism are preserved as inclusions within garnet/clinozoisite and as armored grains in the matrix. The modal amount of amphibole (20%) and plagioclase (15%) has increased at the expense of pyroxene and garnet with increasing metamorphic retrogression. Garnet (40%) in eclogites occurs as porphyroblasts (up to 1.0 cm in diameter), is compositionally zoned and exhibits an inclusion-rich (quartz, amphibole, zoisite and rutile) core overgrown by an inclusion-poor rim. Mineral inclusions can be considered as characteristic mineral phases of the pre-peak stage of metamorphism (FIGURE 8).

Serpentinized peridotites

Serpentinized peridotites show a massive to fragile structure, intense fracturing and high degree of alteration, which is evidenced by the presence of minerals of the serpentine group. It is common to observe the development of sectors with serpentinite showing green in different shades and resinous luster and veinlets of magnetite following and cutting the serpentinite. Carbonate veinlets of white color and matte brightness of up to 0.5 cm thick follow the main foliation of the rock, while those of quartz of white color and glassy brightness of up to 0.2 cm thick cut this foliation almost at right angle. Petrographic analysis reveals that these rocks are serpentinites, which represent rocks generated by secondary alteration of ultrabasic rocks. They consist almost entirely of serpentine group minerals (chrysotile with minor amounts of antigorite), although it is common to find relict minerals of the original rock (peridotite). Pseudomorphic textures, bastites, and fracture fillings are distinguished. The pseudomorphic textures of “mesh” type are characterized by the presence of relict olivine replaced by minerals of the serpentine group (generally chrysotile) along microfractures and grain boundaries, although without development of hourglass type textures as well as textural features before serpentinization. Non-pseudomorphic textures formed by the interpenetration of minerals from the serpentine and even metallic ores (magnetite) are represented by the presence of bastites. Furthermore, textures are observed fracture filling by minerals of the serpentine group.

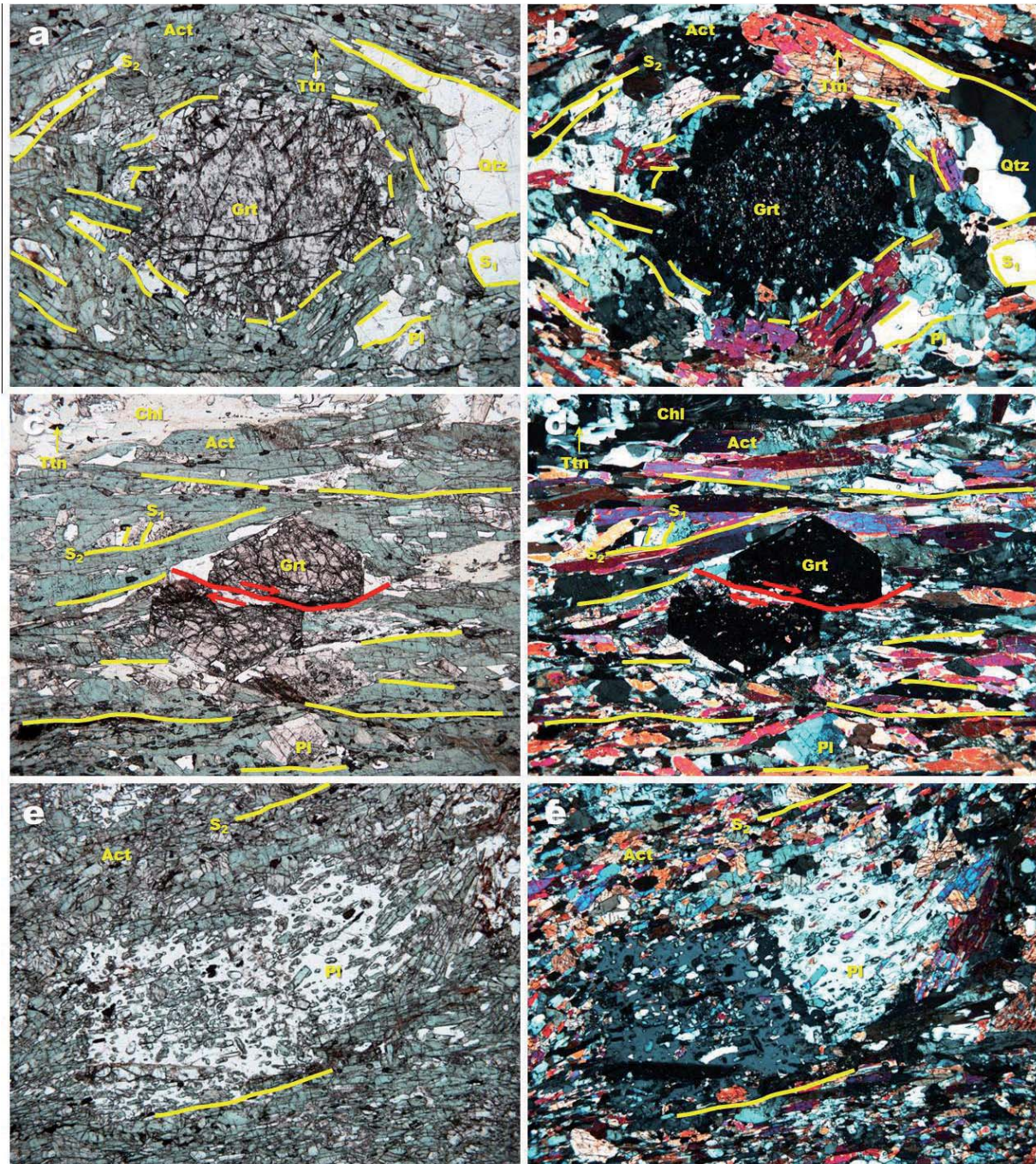


FIGURE 7. Photomicrograph of garnet amphibolites, displaying their main textural and microstructural features. Hbl, hornblende; Pl, plagioclase; Grt, garnet; Qtz, quartz; Ttn, titanite.

Metabasalts

Metabasalts exhibit weak foliation, which is defined by the orientation of the chlorite, and lepidogranoblastic texture. These rocks mainly consist of plagioclase as

the main mineral phase, biotite, quartz and titanite. Plagioclase (54%) forms heteroblastic and xenoblastic individuals, which constitute former phenocrysts or matrix of the protolith. It usually presents polysynthetic

twinning and inclusions of chloritized biotite. Biotite (41%) forms leafy aggregates consisting of heteroblastic and subidioblastic individuals with pleochroism from brown to pale green, and moderate chloritization.

Titanite (5%) individuals occur as granular brown color, which is masked by its birefringence. Quartz form heteroblastic and xenoblastic individuals that develop an old hydrothermal vein.

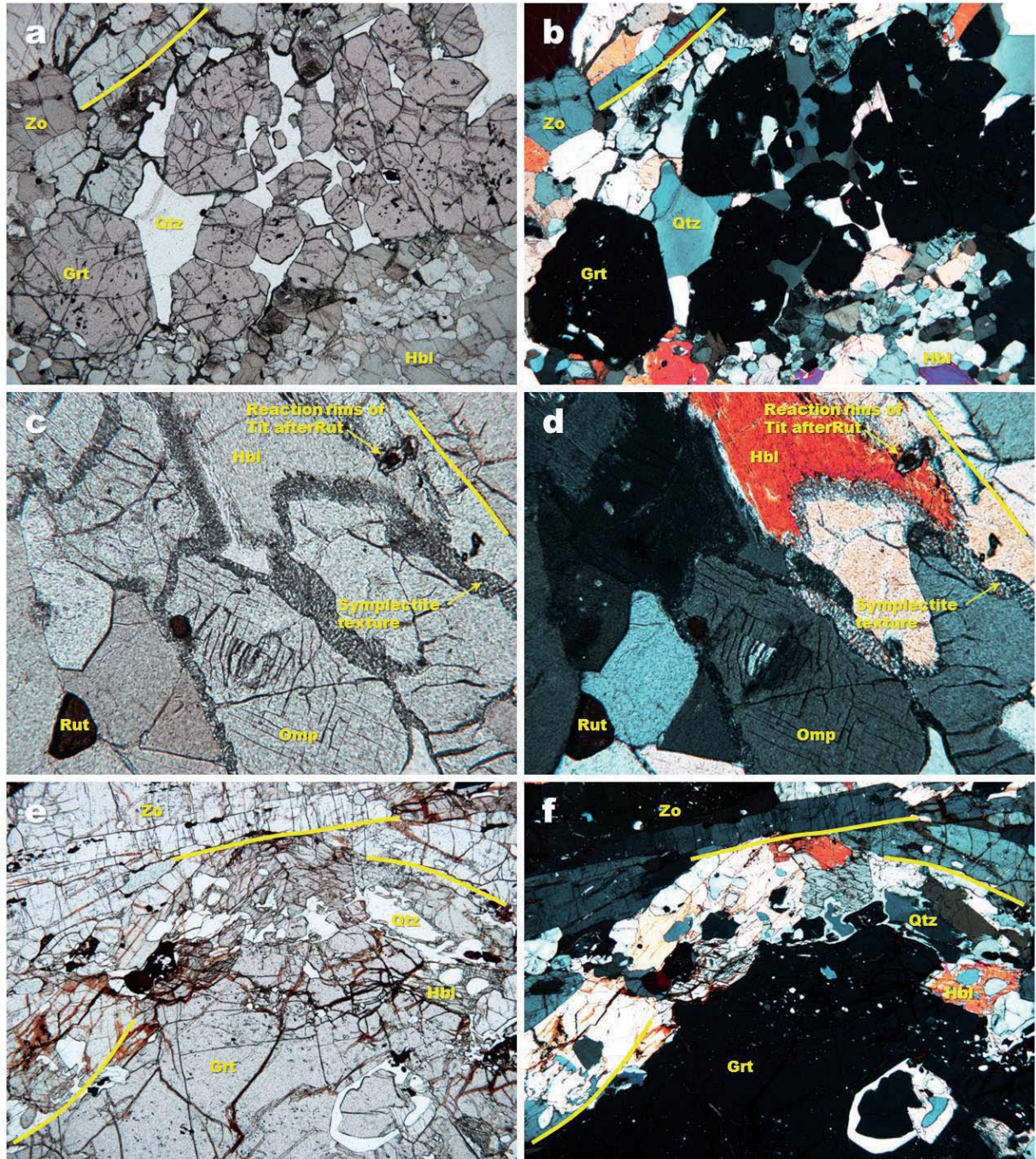


FIGURE 8. Photomicrograph of eclogites, displaying their main textural and microstructural features. Hbl, hornblende; Pl, plagioclase; Zo, zoisite; Grt, garnet; Qtz, quartz; Ttn, titanite; Rut, rutile.

PROGRADE AND RETROGRADE METAMORPHISM

Metabasites of the Arquía Complex were affected by prograde metamorphism, which was followed by a retrograde event after reaching the maximum pressure and temperature conditions. This is based on the following evidences: Field relations between the different lithotypes of metabasites reflect the occurrence of a prograde metamorphism, which is manifested by an increase of metamorphism from the greenschist facies (chlorite and actinolite schists with or without garnet, and metabasalts) to the amphibolite facies (amphibolites with or without garnet). Serpentinized peridotites are tectonically emplaced between actinolite schists and amphibolites. Therefore, the prograde metamorphism of these rocks is marked by the transition from the greenschist facies (chlorite + plagioclase + clinozoisite ± quartz ± titanite ± graphite and actinolite + clinozoisite + quartz + plagioclase ± epidote ± titanite) through the epidote-amphibolite facies (actinolite + hornblende + epidote + clinozoisite + zoisite + quartz + plagioclase ± garnet ± titanite ± rutile ± muscovite) to the amphibolite facies (hornblende + garnet + plagioclase ± quartz). The prograde metamorphism was followed by a retrograde event of metamorphism that partially replaced the mineral assemblages formed during the

peak metamorphic conditions. This is manifested in the characteristic mineralogy of the retrograde mineral assemblages that reached the greenschist facies from typical mineral assemblages of the epidote-amphibolite and amphibolite facies, such as chlorite + actinolite + epidote + clinozoisite + quartz + zoisite + titanite (mineralogy of the greenschist facies) from hornblende + epidote + clinozoisite + zoisite + quartz + albite ± garnet (mineralogy of the epidote-amphibolite facies) in amphibole schists, and chlorite + muscovite + epidote + clinozoisite + zoisite + plagioclase (albite) + titanite + quartz (mineralogy of the greenschist facies) from hornblende + garnet + plagioclase ± quartz (mineralogy of the amphibolite facies) in garnet-amphibolites.

GEOCHEMISTRY

Geochemical studies were performed in actinolite schists (samples ARQ-219, ARQ-231 and ARQ-376), garnet actinolite schists (samples ARQ-171 and ARQ-228), amphibolites (sample ARQ-182) and garnet amphibolites (samples ARQ-181 and ARQ-227). Metabasites geochemically classified as tholeiitic basalts in environments of MORB (N-MORB types). The results of geochemical analysis (TABLE 1) indicate contents of 45.77-49.84 wt% SiO₂, 13.71-15.74 wt% Al₂O₃, and 7.42-9.22 wt% MgO. The K content is very low (0.09 to 0.33 wt%).

TABLE 1. Chemical composition of metabasites of the Arquía Complex.

Sample	ARQ-227	ARQ-231	ARQ-228	ARQ-171	ARQ-181	ARQ-182	ARQ-376	ARQ-219	ARQ-214	ARQ-378	ARQ-379
Lithology	Grt amphibolite	Act schist	Grt bearing act schist	Grt bearing act schist	Grt amphibolite	Amphibolite	Act schist	Act schist	Eclogite	Eclogite	Eclogite
SiO ₂	49.84	48.33	48.13	49.83	45.77	49.03	47.23	49.26	49.30	47.21	49.00
TiO ₂	1.82	1.49	2.24	1.75	1.78	15.6	1.25	1.85	2.39	1.23	1.86
Al ₂ O ₃	13.71	14.16	13.48	14	15.74	3.02	15.57	14.32	13.48	15.17	14.14
Fe ₂ O ₃	3.58	3.24	3.28	3.27	2.73	7.03	3.79	3.56	4.51	2.35	2.73
FeO	8.68	7.68	10.04	9.11	9.35	0.17	6.51	7.98	10.57	7.06	10.24
MnO	0.17	0.16	0.2	0.18	0.21	8.58	0.16	0.18	0.23	0.16	0.20
MgO	7.71	8.57	7.7	7.42	8.64	11.89	9.22	7.66	7.68	7.48	8.39
CaO	9.95	9.88	9.7	9.4	11.83	2.03	11.10	9.94	8.02	13.42	8.95
Na ₂ O	2.55	3.11	2.58	3.72	2.15	0.14	2.50	2.98	2.58	2.35	3.56
K ₂ O	0.2	0.18	0.16	0.15	0.33	0.08	0.05	0.08	0.14	0.20	0.09
P ₂ O ₅	0.18	0.13	0.2	0.14	0.1	1.2	0.12	0.16	0.21	0.10	0.16
LOI	1.4	2.9	2.1	0.8	1.1	0.05	2.3	1.8	0.7	3.1	0.5
Cr ₂ O ₃	0.028	0.044	0.03	0.026	0.069	99.82	0.061	0.029	0.032	0.056	0.027
Total	99.818	99.874	99.84	99.796	99.799	0.1	99.861	99.77	99.842	99.886	99.847
Mo	0.6	0.3	0.6	0.1	0.4	83	0.1	0.3	<0.1	0.6	0.3
NiO	56	74	77	56	180	27.7	79	38	126	96	62
Ni	21.1	31.7	45.9	15.7	104.3	12	33.4	16.0	19.3	54.0	17.0
Zn	19	26	38	17	18	78.3	24	32	24	16	17

Sample	ARQ-227	ARQ-231	ARQ-228	ARQ-171	ARQ-181	ARQ-182	ARQ-376	ARQ-219	ARQ-214	ARQ-378	ARQ-379
Lithology	Grt amphibolite	Act schist	Grt bearing act schist	Grt bearing act schist	Grt amphibolite	Amphibolite	Act schist	Act schist	Eclogite	Eclogite	Eclogite
Cu	25.8	12.6	83	39.9	89.9	0.5	51.6	52.5	33.2	104.8	33.1
As	0.5	0.5	0.5	0.5	3.2	0.1	0.5	0.5	1.2	0.7	<0.5
Cd	0.1	0.1	0.1	0.1	0.1	0.1	0.1	0.1	<0.1	<0.1	<0.1
Sb	0.1	0.1	0.1	0.1	0.1	0.1	0.1	0.1	0.2	0.8	<0.1
Bi	0.1	0.1	0.1	0.1	0.1	0.1	0.1	0.1	<0.1	<0.1	<0.1
Ag	0.1	0.1	0.1	0.1	0.1	0.6	0.1	0.1	<0.1	<0.1	<0.1
Au	2.3	1.1	0.9	0.5	0.5	0.01	0.5	0.5	0.6	<0.5	0.6
Hg	0.01	0.01	0.01	0.01	0.03	0.1	0.01	0.01	0.01	<0.01	<0.01
Tl	0.1	0.1	0.1	0.1	0.1	0.5	0.1	0.1	<0.1	<0.1	<0.1
Se	0.5	0.5	0.5	0.5	0.5	16.1	0.5	0.5	<0.5	<0.5	<0.5
Ga	19.5	16	18.4	18.9	12.8	40	14.5	17.3	18.1	14.3	18.5
Sc	43	42	45	44	43	278	40	42	41	39	44
V	380	336	428	368	272	0.5	285	351	428	263	377
W	0.5	0.5	0.5	0.5	0.5	42.8	1.3	0.5	<0.5	<0.5	<0.5
Co	45	43.4	44.3	44.7	60.1	0.1	35.7	29.8	51.8	45.1	47.6
Cs	0.1	0.1	0.1	0.1	1.2	15	0.1	0.1	0.9	0.3	<0.1
Ba	21	29	19	13	63	2	12	13	22	11	20
Be	2	1	1	1	2	1.7	1	1	2	<1	1
Rb	1.1	0.9	0.5	0.4	6.7	1	0.1	0.1	0.8	2.8	0.3
Sn	1	1	1	1	1	0.2	1	1	2	<1	1
Th	0.2	0.2	0.2	0.2	0.3	0.3	0.2	0.2	<0.2	<0.2	<0.2
Nb	2.4	1.5	2.6	1.9	6.1	0.1	1.0	2.7	3.0	2.5	1.8
Ta	0.2	0.1	0.2	0.2	0.3	130.4	0.1	0.2	0.3	0.1	<0.1
Sr	166.1	113.5	126.6	167.7	99.3	54.1	144.1	167.8	104.4	182.3	109.7
Zr	133.6	90.5	150.3	111.2	117.4	1.7	75.5	114.4	164.2	82.4	117.4
Hf	3.2	2.4	4.3	2.6	2.7	26.5	1.8	3.1	4.6	<0.01	3.5
Y	40.4	34.4	48.4	35.6	25.8	0.1	27.7	39.0	49.3	27.0	41.2
Pb	0.2	0.1	0.4	0.4	0.3	0.1	0.1	0.1	<0.1	0.1	<0.1
U	0.3	0.1	0.4	0.1	0.1	1.7	0.1	0.1	<0.1	<0.1	<0.1
La	4.5	3.0	5.1	3.8	4.6	5.4	3.1	4.7	5.5	3.6	3.8
Ce	13.1	9.1	15.2	11.9	10.9	10.6	8.9	14.3	16.3	10.4	12.8
Pr	2.4	1.74	2.73	2.09	1.76	6.1	1.48	2.47	2.82	1.64	2.18
Nd	13.3	10.5	14.9	11.6	8.6	2.43	8.0	13.6	15.5	8.5	11.5
Sm	4.46	3.61	5.11	3.85	2.8	1.05	2.77	4.53	5.21	2.74	4.24
Eu	1.6	1.4	1.78	1.41	0.75	3.63	1.01	1.57	1.90	1.07	1.50
Gd	5.89	5.17	6.96	5.37	2.75	0.67	3.81	6.10	7.20	4.02	5.69
Tb	1.06	0.89	1.28	0.97	0.47	4.66	0.7	1.07	1.31	0.69	1.05
Dy	7.3	6.26	8.5	6.46	3.59	1.04	4.86	6.65	8.88	4.34	6.95
Ho	1.56	1.32	1.82	1.36	0.9	3.09	1.05	1.49	1.87	0.91	1.52
Er	4.65	3.74	5.52	3.98	3.31	0.45	3.05	4.26	5.38	2.80	4.47
Tm	0.65	0.56	0.86	0.6	0.53	2.66	0.45	0.63	0.85	0.41	0.68
Yb	4.59	3.28	5.64	3.42	3.52	0.43	2.79	4.27	5.62	2.75	4.87
Lu	0.63	0.51	0.77	0.57	0.56		0.45	0.62	0.79	0.40	0.68

The REEs normalized to chondrite C1 (FIGURE 9a) show a higher REE content in garnet metabasites. A slight enrichment of HREEs with respect to LREEs is observed, with a very noticeable Pr enrichment in sample ARQ-181 (garnet amphibolite). The HREEs show an almost flat behavior. An impoverishment in medium REEs in sample ARQ-181 is evident. Most of the samples have a negative anomaly in Eu, which is quite weak in sample ARQ-231 (actinolite schist). The La/Yb (0.63-1.1) and Gd/Yb (0.78-1.67) ratios indicate an igneous protolith. The La/Nb ratio varies between 0.75 and 2.0, being less than 2.5, which is common in oceanic basalts. However, sample ARQ-376 displays a La/Nb ratio of 3.1, slightly higher for

a protolith of oceanic basalt. The patterns of REEs do not differentiate very well schists (samples ARQ-228, ARQ-171, ARQ-231, ARQ-219 and ARQ-376) from amphibolites (samples ARQ-181, ARQ-182 and ARQ-227), which assigns to these rocks a geochemical isotopic signature very similar that is related to a common protolith. The metabasites show a very homogeneous chemical behavior in the N-MORB multi-element spider diagram (FIGURE 9b). The behavior of Nb is flat, without revealing anomalies. A very low content of Ni and a quite enrichment of Y and Sr were observed. The pattern of REE behavior is similar to other metabasites. The most enrichment in all REEs is the sample ARQ-379.

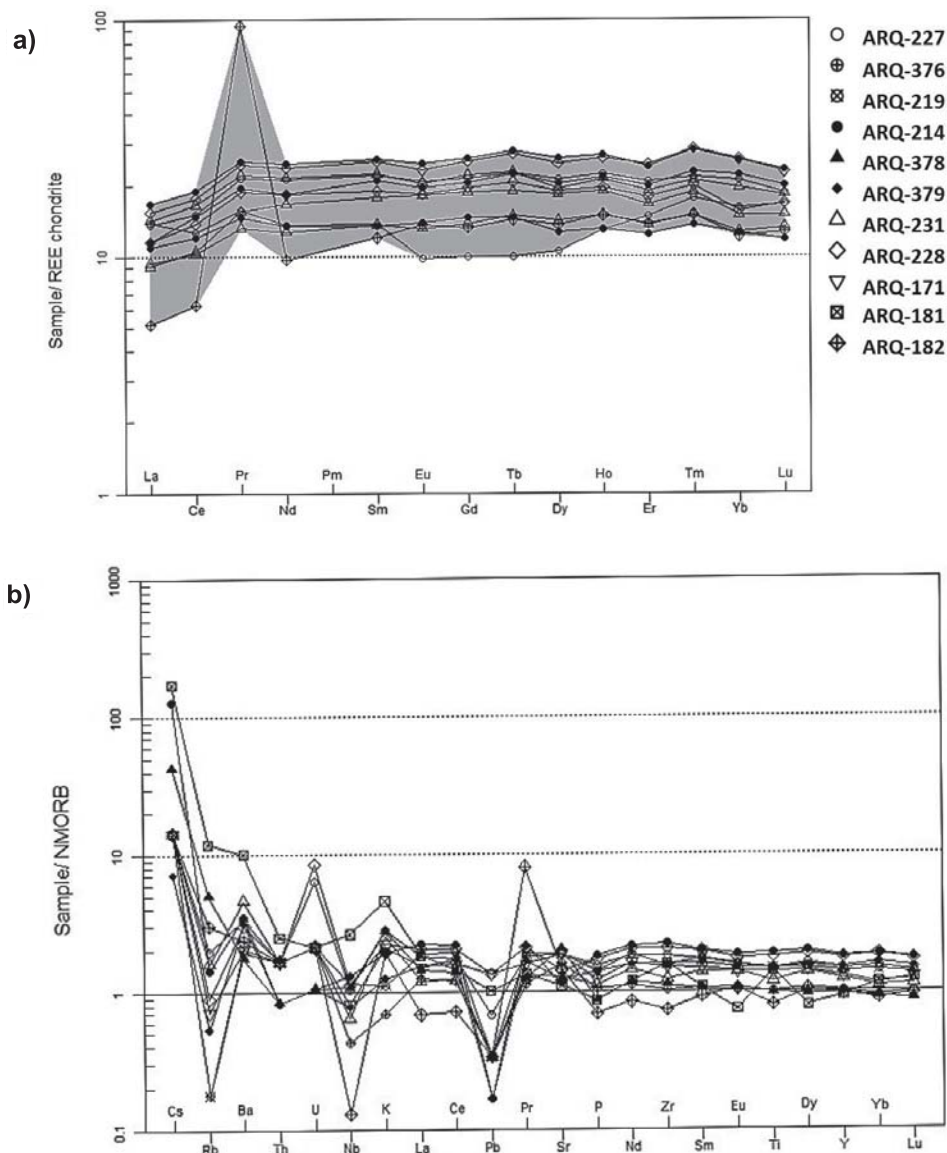


FIGURE 9. a. Chondrite-normalized REE diagram after Nakamura, 1974 and **b.** N-MORB multi-element spider diagram after Sun and McDonough, 1989 of the Arquía Complex metabasites.

The chemical composition of metabasites of the Arquía Complex are plotted in Zr/Ti vs Nb/Y and AFM diagrams as shown in FIGURE 10. The protoliths of

these rocks are located in the boundary between basalt and andesite+basaltic andesite (FIGURE 10a), and in the basalt of tholeiite series (FIGURE 10b).

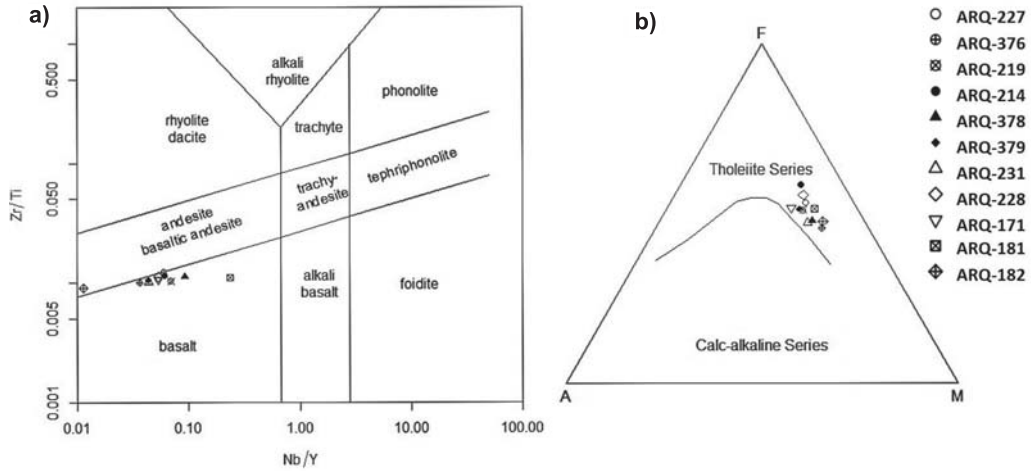


FIGURE 10. Chemical composition of the metabasites of the Arquía Complex expressed in: **a.** Zr/Ti vs Nb/Y diagram of Pearce (1996) and **b.** AFM diagram of Irvine and Baragar (1971).

FIGURE 11 illustrates various tectonic discrimination diagrams after Pearce and Cann (1973). The trace elements analyzed reflect a rise in mid-ocean ridges (MORB) and a protolith of tholeiitic basalts (FIGURE 11a). These diagrams are also useful to know the environment and the protolith of metabasites (FIGURE 11b), which use little mobile trace elements during

the metamorphic processes. Metabasites are located in the field of type MORB basalts (FIGURE 11c). All samples were placed in the field of type MORB basalts. Samples ARQ-228 and ARQ-379 corresponds to a garnet actinole schist and eclogite and are located outside the MORB field, although very near and following the same trend.

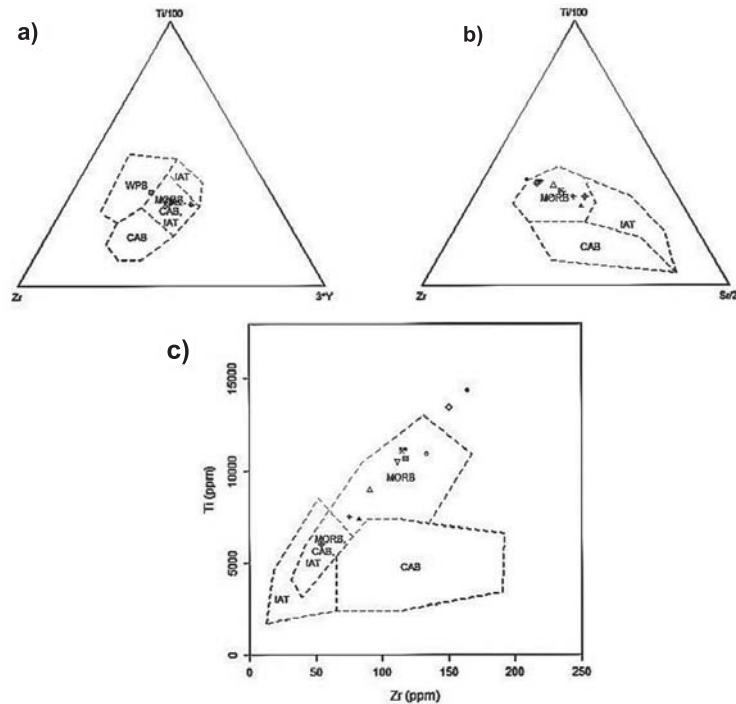


FIGURE 11. Tectonic discrimination diagrams of the Arquía Complex metabasites after Pearce and Cann (1973). **a.** IAT-Island Arc Tholeiites; **b.** CAB-calc-alkali basalts; MORB, CAB and IAT; **c.** WPB-within-plate basalts. Conventions are the same as.

Lu-Hf GEOCHRONOLOGY

Preliminar considerations

The Lu-Hf system has been widely used in recent years as geochronometer, especially for dating the peak of metamorphosis of high pressure and low temperature rocks, such as eclogites and blueschists, among other lithologies (Cheng *et al.*, 2012; Cheng *et al.*, 2015; Peters *et al.*, 2013).

Therefore, this system has become a great tool for dating the growth of garnets in crustal and mantle environments, contributing to elucidate the geodynamic history that has conditioned the geological history of the metamorphic basement of a specific region (Scherer *et al.*, 2001; Cheng *et al.*, 2012; Smit *et al.*, 2013). The closure of the Lu-Hf system in garnet is mostly controlled by the closure of the daughter element to diffusion, which prevents the isotopic reequilibration with garnet with the surrounding matrix (Scherer *et al.*, 2001). Taking into account that Lu-Hf ages obtained in terrains with a usually large polymetamorphic history (but obviously explicable in the context of a temporal and spatial evolution of a specific area), for purposes of specifying the timing of associated metamorphic events, is usually also simultaneously analyzed a sample by using the Sm-Nd system (Cheng *et al.*, 2012; Zirakparvar *et al.*, 2011; Smit *et al.*, 2013). Although in this study, this methodology was followed, unfortunately because of the inability to obtain very clean garnet fractions of for each of the different fractions, the results were not satisfactory (data with errors much higher than the calculated ages). For this reason, the results from the Sm-Nd analyzes were not included in this study. Instead, the best age obtained by the Lu-Hf system is presented, although it is recognized that it also has dispersion higher than what is expected for an isochronous (MSWD < 2.5,

according to documentary justifications by Brooks *et al.* 1972, in a different geochronometer). In the previous context and considering that the age obtained for eclogite analyzed in this study agrees very well with the geological history documented for the area (age with geological significance), particularly with regard to the Arquía Group (Villagómez and Spikings, 2013), we decided to include the best age obtained in this research.

Lu-Hf data

In this study, four fractions of garnet and whole-rock, obtained from the sample ARQ359 (eclogite) were analyzed. The results of the Lu-Hf analysis are summarized in Table 2. The concentrations of Lu and Hf obtained for the whole-rock fractions (ARQ359-WRB1 and ARQ359-WRS1) range between 0.608 to 0.662 ppm and 0.5590 to 2.9586 ppm, respectively, whereas for the garnet fractions (ARQ359-G3 and ARQ359-G4) they vary from 2.217 ppm to 0.1690-0.1716 ppm, respectively. The $^{176}\text{Lu}/^{177}\text{Hf}$ ratios in the whole-rock fractions vary in the range 0.029160-0.168050, with 2σ (abs) values of 0.000146 and 0.000840, respectively. Garnet fractions range from 1.862660 to 1.835050, with 2σ (abs) values of 0.009313 and 0.009175, respectively. The $^{176}\text{Hf}/^{177}\text{Hf}$ ratios in the sub-whole rock samples vary in the range 0.283161-0.283495, with a similar 2σ (abs) value of 0.000016 for both fractions. Garnet fractions range from 0.287544 to 0.287534, with 2σ (abs) values of 0.000018 and 0.000016, respectively. A linear regression for sample ARQ359 (FIGURE 12) using garnet and whole-rock fractions yields a Lu-Hf age of 128.7 ± 3.5 Ma with a Mean Squared Weighted Deviation MSWD (MSWD) = 4.0 and a poorly defined initial $^{176}\text{Hf}/^{177}\text{Hf}$ of 0.283091 ± 0.000083 . The Lu-Hf age obtained for the analyzed sample suggests the age at which it reached the conditions of the eclogite facies during the Barremian (Lower Cretaceous) time.

TABLE 2. Analytical results from this study in garnet and whole-rock fractions.

Sample	Concentrations			Lu ratios			Interferences			Data to project			
	sp. Wt.	Lu (ppm)	Hf (ppm)	$^{176}\text{Lu}/^{175}\text{Lu}$	$^{175}\text{Lu}/^{177}\text{Hf}$	$^{173}\text{Yb}/^{177}\text{Hf}$	$^{176}\text{Lu}/^{177}\text{Hf}$	$^{176}\text{Hf}/^{177}\text{Hf}$	Error	$^{176}\text{Lu}/^{177}\text{Hf}$	2s (abs)	$^{176}\text{Hf}/^{177}\text{Hf}$	2s (abs)
ARQ359 G3	0.12303	2.2170	0.1690	0.129003	0.000014	0.000026	1.862660	0.287544	0.000011	1.862660	0.009313	0.287544	0.000018
ARQ359 G4	0.12430	2.2170	0.1716	0.135952	0.000059	0.000025	1.835050	0.287534	0.000008	1.835050	0.009175	0.287534	0.000016
ARQ359 WRB1	0.09587	0.6080	29.586	0.239307	0.000000	0.000003	0.029160	0.283161	0.000007	0.029160	0.000146	0.283161	0.000016
ARQ359 WRS1	0.02724	0.6620	0.5590	0.084063	0.000001	0.000000	0.168050	0.283495	0.000007	0.168050	0.000840	0.283495	0.000016

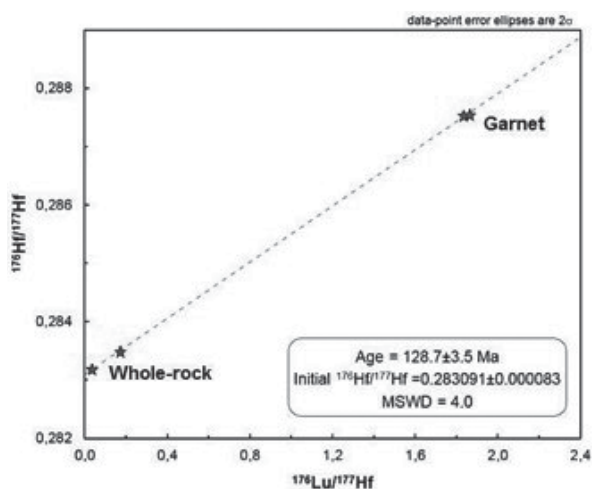


FIGURE 12. Lu-Hf errorchron diagram for sample ARQ359 (eclogite) from the Arquía Complex. The 128.7 ± 3.5 Ma age results from regression all the garnet and whole-rock fractions together.

DISCUSSION AND RESULTS

In the Romeral Melange of Cedié *et al.* (2003) discontinuous and thin tectonic blocks of oceanic and continental origin are located (Rodríguez and Arango, 2013). Different geochemical studies of the Complex Arquía rocks are in agreement with an oceanic origin from tholeiitic basalts in MORB- or N-MORB-type environments (Villagómez *et al.*, 2011; Rodríguez and Arango, 2013). The behavior of REEs show a depletion in LREEs and a nearly flat bit fractional behavior of the HREEs with similar relations for

the $(La/Sm)_N < 0.6$ with absence of negative anomalies in Nb, Ta and Ti. According Villagómez *et al.* (2011), this can be associated with a subduction process. Rodríguez and Arango (2013), taking into account the lithological association between deformed metabasites, scarce metapelites and ultramafic rocks, suggest that Complex Arquía rocks can constitute remnants of an ophiolite sequence of the N-MORB-type series. The Lu-Hf age obtained in the present study (128.7 ± 3.5 Ma) corresponds with the age range in which the roll-back process of the slab that took place while it was subducting below the continental margin of South America (Spikings *et al.*, 2015), and whose composition must be fundamentally basic (protolith of the Arquía Group). This roll-back process largely occurred due to the aforementioned eclogitization, considering that this transformation involves an increase in the density of subducting materials (becoming higher even than the density of mantle rocks). In this regard, it is worth noting that the density of a basaltic rock (approximate composition of the protolith of the Arquía Group) is usually about 2.9 g/cm^3 , while the density of an eclogite is usually $> 3.4 \text{ g/cm}^3$ (Carmichael, 1989), *i.e.* an eclogite reaches a higher density than mantle rocks ($\sim 3.23 \text{ g/cm}^3$, according to Cloos, 1993). The referred roll-back process consequently relates to the formation of an intra-oceanic arc that took place very close to the continent (the Quebradagrande magmatic arc of Spikings *et al.*, 2015), due to the expansion in the supra-subduction area (resulting from the contemporary process of roll-back), which took place when the rocks of the subducting slab were transformed to eclogite (FIGURE 13).

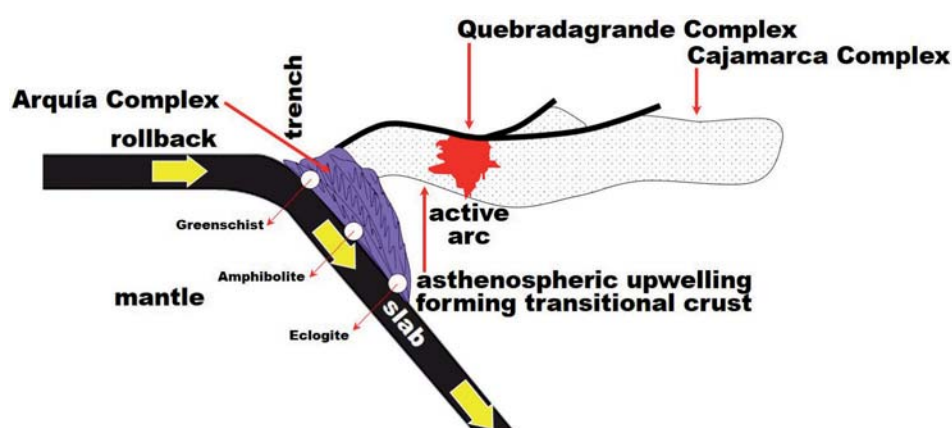


FIGURE 13. Schematic diagram illustrating the position of the Arquía, Quebradagrande and Cajamarca Complexes for the interval 141-115Ma. Modified from Spikings *et al.* (2015).

ACKNOWLEDGEMENTS

This study was funded by the Universidad Industrial de Santander through research project 5464 (Petrogenesis of metamorphic rocks of the Arquía Complex in

the Córdoba-Pijao-Génova sector, Quindío, Central Cordillera, Colombia). We are grateful to students of the School of Geology for their help with the fieldwork. We are indebted to this institution for allowing us the use of research facilities. Discussions with members

of the Research Group in Basic and Applied Geology of the Universidad Industrial de Santander aided our understanding on the geology of the Arquía Complex. The authors also acknowledge to Dr Luz Mary Toro and Dr. Idael Blanco for their critical and insightful reading of the manuscript and are most grateful to the above-named people and institutions for support.

REFERENCES

- AcmeLabs 2015. Price Brochure. Consultado el 13 de marzo de 2016. http://acmelab.com/pdfs/Acme_Price_Brochure.pdf.
- Bouvier, A., Vervoort, J.D., and Patchett, P.J. 2008. The Lu–Hf and Sm–Nd isotopic composition of CHUR: Constraints from unequilibrated chondrites and implications for the bulk composition of terrestrial planets. *Earth and Planetary Science Letters*, 273(1-2): 48-57.
- Brooks, C., Hart, S.R., and Wendt, I. 1972. Realistic use of two-error regression treatments as applied to rubidium–strontium data. *Reviews of Geophysics*, 10(2): 551-577.
- Bustamante, A., Juliani, C., Hall, C.M., and Essene, E.J. 2011. ⁴⁰Ar/³⁹Ar ages from blueschists of the Jambaló region, Central Cordillera of Colombia: implications on the styles of accretion in the Northern Andes. *Geologica Acta*, 9(3-4): 351-362.
- Carmichael, R.S. 1989. CRC practical handbook of physical properties of rocks and minerals. CRC Press, Boca Raton, FL. 741p.
- Cheng, H., King, R.L., Nakamura, E., Vervoort, J.D., and Zhou, Z. 2008. Coupled Lu–Hf and Sm–Nd geochronology constrains garnet growth in ultra-high-pressure eclogites from the Dabie orogen. *Journal of Metamorphic Geology*, 26(7): 741-758.
- Cheng, H., Zhang, C., Vervoort, J.D., Li, X., Li, Q., Wu, Y., and Zheng, S. 2012. Timing of eclogite facies metamorphism in the North Qinling by U–Pb and Lu–Hf geochronology. *Lithos*, 136-139: 46-59.
- Cheng, H., Liu, Y., Vervoort, J.D., and Lu, H. 2015. Combined U–Pb, Lu–Hf, Sm–Nd and Ar–Ar multichronometric dating on the Bailang eclogite constrains the closure timing of the Paleo-Tethys Ocean in the Lhasa terrane, Tibet. *Gondwana Research*, 28(4): 1482-1499.
- Cediel, F., Shaw, R.P., and Cáceres, C. 2003. Tectonic assembly of the Northern Andean Block. In: Bartolini, C., Buffler, R.T., and Blickwede, J. (eds.). *The Circum-Gulf of Mexico and the Caribbean: Hydrocarbon habitats, basin formation, and plate tectonics*. AAPG Memoir, 79: 815-848.
- Cloos, M. 1993. Lithospheric buoyancy and collisional orogenesis: subduction of oceanic plateaus, continental margins, island arcs, spreading ridges, and seamounts. *Geological Society of America Bulletin*, 105(6): 715-737.
- Irvine, T.N., and Baragar, W.R.A. 1971. A guide to the chemical classification of the common volcanic rocks. *Canadian Journal of Earth Sciences*, 8(5): 523-548.
- Janoušek, V., Farrow, C.M., and Erban, V. 2006. Interpretation of whole-rock geochemical data in igneous geochemistry: introducing Geochemical Data Toolkit (GCDkit). *Journal of Petrology*, 47(6): 1255-1259.
- Kerr, A., Marriner, G., Tarney, J., Nivia, A., Saunders, A., Thirlwall, M., and Sinton, C. 1997. Cretaceous basaltic terranes in western Colombia: Elemental, chronological and Sr–Nd isotopic constraints on petrogenesis. *Journal of Petrology*, 38(6): 667-702.
- Ludwig, K.R. 2003. User's Manual for Isoplot 3.00: A Geochronological Toolkit for Microsoft Excel. Berkeley Geochronology Center Special Publication, Berkeley.
- Maya, M., y González, H. 1995. Unidades litodémicas en la Cordillera Central de Colombia. *Boletín Geológico, INGEOMINAS*, 35: 43-57.
- McCourt, W., Aspden, J., and Brook, M. 1984. New geological and geochronological data from the Colombia Andes: continental growth by multiple accretion. *Journal of the Geological Society, London*, 141: 831-845.
- McCourt, W., Mosquera, D., Nivia, A., y Núñez, A. 1985. Reseña explicativa del mapa geológico preliminar plancha 243 Armenia, escala 1:100.000. Instituto Colombiano de Geología y Minería, 16p.
- Moreno-Sanchez, M., and Pardo-Trujillo, A. 2003. Stratigraphical and sedimentological constraints on western Colombia: Implications on the evolution of the Caribbean plate. In: Bartolini, C., Buffler, R.T., and Blickwede, J. (Eds.). *The Circum-Gulf of Mexico and*

- the Caribbean: Hydrocarbon habitats, basin formation, and plate tectonics. *AAPG Memoir Vol. 79*: 891-924.
- Münker, C., Weyer, S., Scherer, E., and Mezger, K. 2001. Separation of high field strength elements (Nb, Ta, Zr, Hf) and Lu from rock samples for MC-ICPMS measurements. *Geochemistry, Geophysics, Geosystems*, 2(12):1-19.
- Nakamura, N. 1974. Determination of REE, Ba, Fe, Mg, Na and K in carbonaceous and ordinary chondrites. *Geochemical and Cosmochemical Acta*, 39: 757-773.
- Nesheim, T.O., Vervoort, J.D., McClelland, W.C., Gilotti, J.A., and Lang, H.M. 2012. Mesoproterozoic syntectonic garnet within Belt Supergroup metamorphic tectonites: Evidence of Grenville-age metamorphism and deformation along northwest Laurentia. *Lithos*, 134-135: 91-107.
- Patchett, P.J., and Tatsumoto, M. 1981. A routine high-precision method for Lu-Hf isotope geochemistry and chronology. *Contributions to Mineralogy and Petrology*, 75(3): 263-267.
- Pearce, J.A., and Cann, J.R. 1973. Tectonic setting of basic volcanic rocks determined using trace element analyses. *Earth Planetary Science Letters*, 19(2): 290-300.
- Pearce, J.A. 1996. A user's guide to basalt discrimination diagrams. In: Wyman, D. A. (ed.) *Trace element geochemistry of volcanic rocks: Applications for massive sulphide exploration*. Geological Association of Canada, Short Course Notes, Vol. 12. pp. 79-113.
- Peters, T.J., Ayers, J.C., Gao, S., and Liu, X.M. 2013. The origin and response of zircon in eclogite to metamorphism during the multi-stage evolution of the Huwan Shear Zone, China: Insights from Lu-Hf and U-Pb isotopic and trace element geochemistry. *Gondwana Research*, 23(2): 726-747.
- Pindell, J., and Kennan, L. 2009. Tectonic evolution of the Gulf of Mexico, Caribbean and northern South America in the mantle reference frame: an update. *Geological Society of London, Special Publications*, 328: 1-55.
- Rodríguez, G., y Arango, M. 2013. Reinterpretación geoquímica y radiométrica de las metabasitas del Complejo Arquía. *Boletín de Geología*, 35(2): 65-81.
- Ruiz, E., Blanco, I., Toro, L., Moreno, M., Vinasco, C., García, A., Morata, D., and Gómez, A. 2012. Geoquímica y petrología de las metabasitas del Complejo Arquía (Municipio de Santafé de Antioquia y Río Arquía, Colombia): Implicaciones geodinámicas. *Boletín Ciencias de la Tierra*, 32: 65-80.
- Ruiz, E. 2013. Geoquímica y trayectorias PT de las rocas metamórficas del Complejo Arquía, entre los municipios de Santafé de Antioquia (Antioquia) y el río Arquía (Caldas). Tesis de Maestría, Universidad de Caldas, Manizales, 109p.
- Scherer, E.E., Münker, C., and Mezger, K. 2001. Calibration of the Lutetium-Hafnium clock. *Science*, 293: 683-686.
- Smit, M.A., Scherer, E.E., and Mezger, K. 2013. Lu-Hf and Sm-Nd garnet geochronology: Chronometric closure and implications for dating petrological processes. *Earth and Planetary Science Letters*, 381: 222-233.
- Söderlund, U., Patchett, P., Vervoort, J.D., and Isachsen, C.E. 2004. The ^{176}Lu decay constant determined by Lu-Hf and U-Pb isotope systematic of Precambrian mafic intrusions. *Earth and Planetary Science Letter*, 219(3-4): 311-324.
- Spikings, R., Cochrane, R., Villagómez, D., Lelij, R., Vallejo, C., Winkler, W., and Beate, B. 2015. The geological history of northwestern South America: from Pangea to the early collision of the Caribbean Large Igneous Province (290-75 Ma). *Gondwana Research*, 27(1): 95-139.
- Sun, S.S., and McDonough, W.F. 1989. Chemical and isotopic systematics of oceanic basalts: implications for mantle composition and processes. In: *Magmatism in the Ocean Basins*, Saunders, A.D. and Norry, M.J., eds. Geological Society of London, Special Publications, 42: 313-345.
- Toussaint, J.F., y Restrepo, J.J. 1978. Edad cretácea de una anfibolita granatífera de Pijao, Quindío. *Publicación Especial de Geología*, Universidad Nacional de Colombia, 17: 1-2.
- Vervoort, J.D., and Patchett, P.J. 1996. Behavior of hafnium and neodymium isotopes in the crust: Constraints from Precambrian crustally derived granites. *Geochimica et Cosmochimica Acta*, 60(19): 3717-3723.

Vervoort, J.D., Patchett, P.J., Söderlund, U., and Baker, M. 2004. Isotopic composition of Yb and the determination of Lu concentrations and Lu/Hf ratios by isotope dilution using MC-ICPMS. *Geochemistry, Geophysics, Geosystems*, 5(11):1-15

Villagómez, D. 2010. Thermochronology, geochronology and geochemistry of the Western and Central cordilleras and Sierra Nevada de Santa Marta, Colombia: The tectonic evolution of NW South America. Thèse de doctorat, Faculté Des Sciences, Département de Minéralogie, Genève, Université de Genève, Switzerland, 126p.

Villagómez, D., Spikings, R., Magna, T., Kammer, A., Winkler, W., and Beltrán, A. 2011. Geochronology, geochemistry and tectonic evolution of the Western and Central Cordilleras of Colombia. *Lithos*, 125(3-4): 875-896.

Villagómez, D., and Spikings, R. 2013. Thermochronology and tectonics of the Central and Western Cordilleras of Colombia: Early Cretaceous–Tertiary evolution of the Northern Andes. *Lithos*, 160-161: 228-249.

Whitney, D.L., and Evans, B.W. 2010. Abbreviations for names of rock-forming minerals. *American Mineralogist*, 95: 185-187.

Zirakparvar, N.A., Baldwin, S.L., and Vervoort, J.D. 2011. Lu–Hf garnet geochronology applied to plate boundary zones: Insights from the (U)HP terrane exhumed within the Woodlark Rift. *Earth and Planetary Science Letters*, 309(1-2): 56-66.

Received: 13 September 2016

Accepted: 22 November 2016

Manuscript published online: diciembre 05 de 2016